Experimental targeting and control of spatiotemporal chaos in nonlinear optics

L. Pastur, L. Gostiaux, U. Bortolozzo, S. Boccaletti and P.L. Ramazza
Istituto Nazionale di Ottica Applicata, Largo E. Fermi 6, 50125 Firenze, Italy
(Dated: February 8, 2008)

We demonstrate targeting and control over spatiotemporal chaos in an optical feedback loop experiment. Different stationary target patterns are stabilized in real-time by means of a two dimensional space extended perturbation field driven by an interfaced computer and applied in real-space to a liquid crystal display device inserted within a control optical loop. The flexibility of the system in switching between different target patterns is also demonstrated.

PACS: 05.45.Gg,05.45.Jn,42.65.Sf,47.54.+r

Control of complex dynamics refers to a process whereby the critical sensitivity of such dynamics to external disturbances is capitalized in order to select a proper tiny perturbation able to attain a desirable target behavior. In the last decade, a series of relevant issues such as stabilizing a given trajectory within an infinite set of unstable periodic orbits embedded within a chaotic attractor (*control of chaos*) or bringing a chaotic trajectory to a small neighborhood of some desired locations in phase space (*targeting of chaos*) have been addressed and solved in both low and high dimensional time-chaotic dynamics [1].

More recently, the interest switched to implementing control strategies for the stabilization of space-time chaotic dynamics occurring in extended systems. In this latter framework, some theoretical attempts and numerical demonstrations have been offered for achieving control over one and two dimensional patterns [2], coupled map lattices and arrays of oscillators [3], or relevant model equations describing universal features of systems closeby to space time bifurcations, such as the Complex Ginzburg Landau Equation [4] and the complex Swift-Hohenberg Equation [5].

Robust and reliable experimental control over space time chaos (STC) remains however an open problem. In the field of nonlinear optics, a few experimental demonstrations of pattern control and targeting have been offered, based on Fourier filtering techniques [6, 7]. These methods provide a nice efficiency for the stabilization of stationary patterns with global symmetries, but their application to target patterns involving complex phase relationships among different Fourier components (such as localized patterns or selected snapshots of STC evolving patterns) is strongly limited by the practical difficulty of building suitable Fourier masks.

In this Letter we show the first experimental evidence of control of STC based upon a real-space real-time feedback technique, which is able to circumvent the above difficulties, thus allowing stabilization and targeting of two dimensional stationary patterns with arbitrary symmetries and shapes. This is realized by means of perturbing fields applied directly in the real-space and in times shorter than the characteristic time of the pattern dynamics, so that stationary non-homogeneous patterns of arbitrary complexity in space can be indifferently targeted and stabilized with good efficiency. We furthermore show that our control strategy offers dynamical flexibility in switching from one to another target pattern, without the need of removing optical components (as e.g. filters) in the control loop.

The experimental setup is sketched in Fig. 1a. It consists of a main optical feedback loop (MOFL) hosting a Liquid Crystal Light Valve (LCLV) [8], and of an additional electrooptic control loop. The latter is essentially constituted by a videocamera, a personal computer driving a liquid crystal display (LCD), and a laser beam which traverses the LCD before being injected into the MOFL. The LCLV operates as a Kerr-like medium, i.e., it induces on the reading light a phase delay proportional to the writing intensity, over a wide range of input intensities. This proportionality relation holds for the experimental parameters used in the present investigation. The LCD display, operating in transmission, encodes linearly the gray level images output by the PC, onto the laser beam traversing it.

When the control loop is open, a homogeneous wave is sent onto the front face of the LCLV, and is reflected acquiring a spatial phase modulation. The beam propagates within the MOFL from the front face of the LCLV to the input plane of a fiber bundle, experiencing diffraction, and thus converting phase into amplitude modulations. The fiber bundle FB just relays the intensity distribution from the input to the output plane, which is in contact with the LCLV rear face.

In these conditions, the dynamics within the MOFL is described by the equation [9, 10]:

$$\frac{\partial \phi}{\partial t} = -\frac{1}{\tau}(\phi - \phi_0) + D\nabla^2\phi + \alpha I_{fb}, \qquad (1)$$

where $\phi(x, y)$ is the phase of the optical beam at the output of the valve, τ is a relaxation time, D a diffusion coefficient, α the nonlinearity strength of the LCLV, ϕ_0 is the working reference phase, and $I_{fb}(x, y)$ is the feedback intensity impinging at the rear side of the valve.

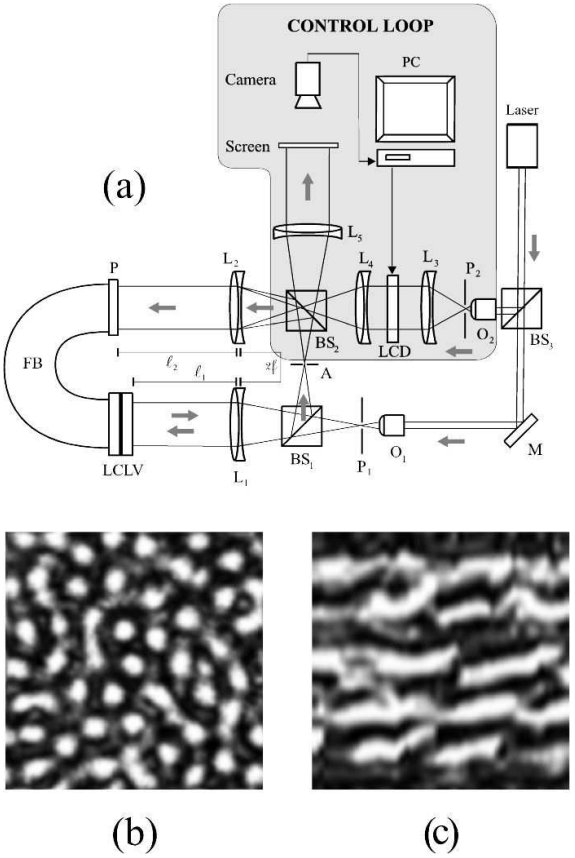

FIG. 1: a) Experimental setup. Main loop: an extended laser beam is closed through a non-linear Kerr-like medium (liquid crystal optical valve). Instabilities develop in the transverse plane of the beam. M: mirror, O_1: microscope objectives; P_1: pinhole; A: aperture; BS_1, BS_2: beam splitters; LCLV: liquid crystal light valve; L_1, L_2: lenses of focal lens f; L_5: additional lens; FB: fiber bundle. In our experiment, $2f-(l_1+l_2)=+90$ mm. Control arm: O_2: microscope objectives; P_2: pinhole; BS_3: beam splitters; LCD: liquid crystal display; L_3, L_4: lenses. The arrows indicate the local direction of light propagation. b) Snapshot of the uncontrolled STC state obtained for an input intensity $I/I_c \sim 3.2$ (I_c being the critical value for pattern formation from the uniform state to hexagons). The pattern intensity has been coded into a 256 levels gray scale. c) Space (vertical)-time (horizontal) dynamical evolution of the central vertical line of pixels of Fig. 1b.

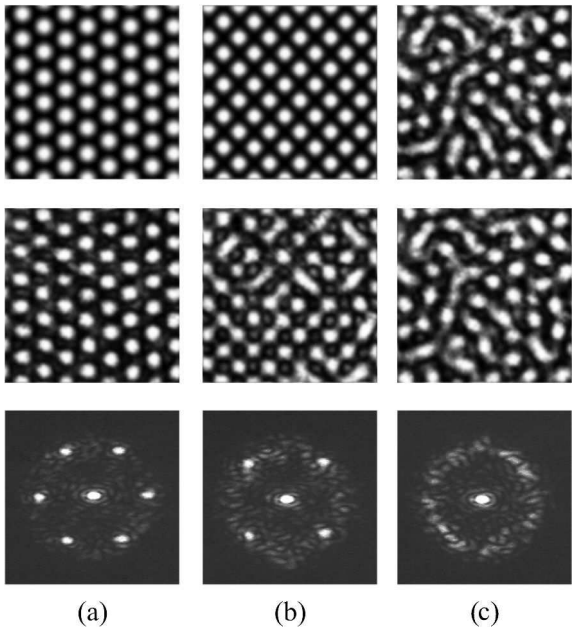

FIG. 2: Examples of target patterns (top row), controlled area in the system at $\gamma = 0.4$ (center row) and corresponding far field images (bottom row) for the control trials of a perfect hexagonal pattern (a), a square pattern (b), and a snapshot of the uncontrolled dynamics (c).

The feedback intensity, which results from the propagation of the beam reflected by the front side of the valve trough the MOFL, is a nonlinear (and nonlocal) function of the phase ϕ [9, 10]. On increase of the pump intensity I, the homogeneous solution destabilizes, resulting in hexagonal patterns close to threshold. If the pump is further increased, regular hexagons loose stability in favour of a space-time chaotic dynamics [9, 11]. Together with the pump value, another parameter of the utmost importance is the spatial frequency bandwidth of the system [7], controlled by the aperture A in Fig. 1. Troughout the present paper, this bandwidth is kept fixed at $\simeq 1.3$ times the diffractive wavenumber of the system, which gives the scale of the unstable structures.

In order to achieve control over the dynamics, a fraction of the beam traveling on the MOFL is extracted and detected by a videocamera, which is interfaced to the PC via a frame grabber. The computer processes the input image, and sends a suitable driving signal to the liquid crystal display device. The LCD transfer function $T(x,y)$ can be written as the contribution of a constant mean transfer coefficient T_0, plus a modulation signal $s(x,y)$. This modulation s is chosen to be proportional to the error signal between the current pattern intensity I_{fb} present in the system, and a target pattern $I_T(x,y)$:

$$s(x,y,t) = -\beta\left(I_{fb}(x,y,t) - I_T(x,y)\right). \qquad (2)$$

The digital processing operations performed by the PC include the evaluation of the above error signal, and the calculation of the cross-correlation between pattern and target. The entire time series of pattern is also recorded on the hard disk for further off-line processing.

The resulting refreshing time for the above procedure is at most 200 ms, to be compared with the characteristic time of the pattern dynamics (computed from the decay of the autocorrelation function) which is of the order of the second.

The LCD is illuminated with a uniform intensity I_0, and the output beam is imaged onto the rear (writing)

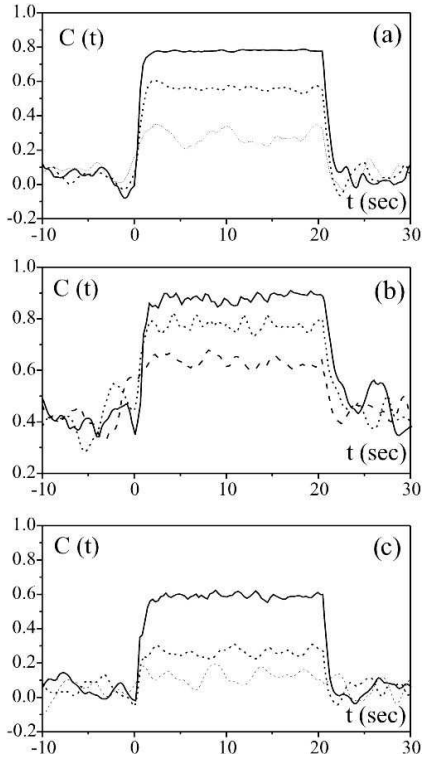

FIG. 3: Correlation function $C(t)$ (a,c,e) and amount of power $p(t)$ injected within the control arm (b,d,f) *vs.* time (in sec.). The two quantities are defined in the text. In all cases the continuous line refers to $\gamma = 0.4$, the dotted line to $\gamma = 0.2$, and the dashed line to $\gamma = 0.1$. (a,b) the target is a perfect hexagonal pattern; (c,d) the target is a snapshot of the uncontrolled dynamics; (e,f) the target is a perfect square pattern. $I/I_c \simeq 3.2$.

side of the valve. Following the above discussion, this beam will consist of a constant term $T_0 I_0$ that acts in renormalizing the valve working point ϕ_0 to $\phi_0{}'$, plus a modulated controlling beam sI_0.

The equation of motion when the control loop is closed is therefore:

$$\frac{\partial \phi}{\partial t} = -\frac{1}{\tau}(\phi - \phi_0') + D\Delta\phi + \alpha\left(I_{fb} - \gamma(I_{fb} - I_T)\right). \quad (3)$$

where $\gamma \equiv \beta I_0$.

We initially set the light intensity at the input of the feedback loop to be $I/I_c \sim 3.2$, where I_c is the critical value for pattern formation from the uniform state to hexagons. In these conditions, the uncontrolled evolution brings the system to display a time evolving, spatially disordered pattern, where many defects are continuously created and annihilated within an hexagonal-like pattern, thus generating STC [11]. A typical snapshot of the uncontrolled dynamics is reported in Fig. 1b. Fig. 1c reports the space-time dynamical evolution of the central vertical line of pixels in Fig. 1b, showing how the uncontrolled dynamics evolves within STC, with a non

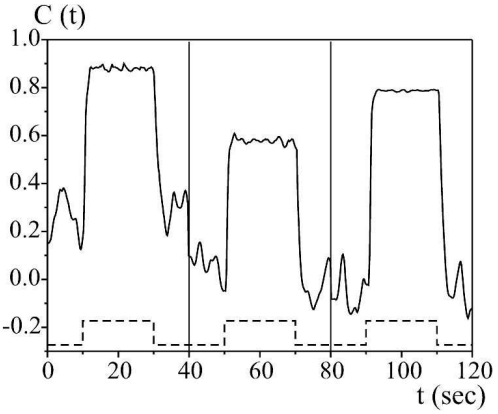

FIG. 4: Correlation function $C(t)$ (see text for definition) *vs.* time during the sequential control trial at $\gamma = 0.4$. The target patterns are a snapshot of the uncontrolled dynamics ($10 \le t < 30$ sec.), a square pattern ($50 \le t < 70$ sec.) and a hexagonal pattern ($90 \le t < 110$ sec.). The dashed line indicates the switching on/off times. The vertical lines separates the three domains in time in which a different pattern is taken as target for the control. In each time domain, the correlation is calculated using the corresponding target pattern.

stationary complex local dynamics and a decaying spatial correlation.

Starting from these conditions, three different target patterns are selected, namely perfect hexagons, squares and a particular snapshot of the uncontrolled dynamical evolution (shown in the top row of Fig. 2).

Perfect stationary hexagons are a stable solution close to the pattern formation threshold; they are destabilized when the pump is increased, resulting in the space-time chaotic dynamics here considered. Therefore, use of hexagons as a target tests the ability of the method to control an unstable solution.

On the other hand, using as target a snapshot of the uncontrolled dynamics assesses the robustness of the method to freeze a given natural state of the uncontrolled dynamics, in the very same spirit as the so called targeting of chaos [1]. Finally, squares are never spontaneously selected by the system without control, and therefore they serve us to assess the ability of the control strategy to force the appearance of an arbitrary symmetry. The results obtained for $\gamma = 0.4$ in the three cases are reported in the center row of Fig.2, indicating that the control procedure is successful in all cases. The patterns are conveniently stabilized over a selected area of 128×128 pixels (about 10 pattern wavelengths) in the system. The bottom row of Fig.2 shows the far field images of the controlled dynamics. While hexagonal and square patterns have a rather simple global symmetry (thus allowing for an easy implementation of Fourier filtering techniques, like the one of Ref. [6]), the target STC snapshot involves the presence of a complicate power spectrum. The fabrication of Fourier masks reproducing the amplitude

and phase of these patterns appears extremely difficult in experiments.

Our control method circumvents such practical difficulties, and effectively stabilizes such complex Fourier patterns. Hence, it configures as the most reliable choice for the stabilization and targeting of two dimensional stationary structures with arbitrary symmetries and shapes.

To evaluate quantitatively the control ability of our method, we use the time dependent correlation function $C(t) =< I_{fb}(\mathbf{r},t) \cdot I_T(\mathbf{r}) >_{\mathbf{r}}$ between the instantaneous pattern and the target one ($< ... >_{\mathbf{r}}$ denotes a spatial average). We also measure the amount of power $p(t) = \gamma[< (I_{fb}(\mathbf{r},t) - I_T(\mathbf{r}))^2 >_{\mathbf{r}}]^{1/2}$ injected within the control arm for controlling the target pattern.

The correlations *vs* time are shown in Fig.3 for increasing values of γ for the control task of a perfect hexagonal pattern (a), a snapshot of the uncontrolled dynamics (b), and a square pattern (c). At lower values of γ ($\gamma = 0.1, 0.2$), there is already a partial control of the dynamics, though several deviations of the patterns around the target ones still remain. This is reflected by the rather large fluctuations of $C(t)$ visible in Fig. 3. The correlation value increases with γ up to $\gamma = 0.4$, when a high degree of control is achieved in all cases. As γ increases, the transient time before reaching control over the target pattern decreases. On the opposite, when control is switched off, the relaxing time is determined by the characteristic time of the STC decorrelation, and is therefore independent of γ. The value of the control power $p(t)$ needed to achieve control is in the range $0.1 - 0.2$ for the data reported.

Notice that the maximum correlation is attained for the case of the STC snapshot. This is due to the fact that in this case the target pattern is a specific configuration of the natural evolution of the dynamics. In the cases of squares and hexagons, instead, the target patterns are are digitally generated trying to reproduce at best the natural profile of the spots present in the system; but this procedure is intrinsically imperfect, because the exact profile of the spots is unknown. The mismatch between the profiles of the targets and the patterns lowers the correlation levels, with respect to the values that would be obtainable in the ideal case, in which the profile of the solution is perfectly reproduced by the target image.

It is worth observing that the correlation when control is off in Fig. 3c does not decay to zero; this is due to the fact that our uncontrolled STC dynamics gives rise to a non zero mean field. This point can be qualitatively appreciated from inspection of Fig. 1c: the pattern has a certain degree of "phase rigidity", i.e., even if there are chaotic fluctuations, bright (dark) areas remain more or less bright (dark) for most of time. Similar properties have been observed experimentally and discussed in various other cases of space extended systems giving rise to STC dynamics [12].

Finally, we demonstrate that our control technique is greatly flexible in dynamically switching between different target patterns. For this purpose, we prepare a time-dependent target pattern formed by the ordered sequence of a snapshot of the uncontrolled dynamics, a square pattern and a hexagonal pattern, each one presented to the system for a time $T = 20$ sec., and intermingled with periods of $T = 20$ sec. of time in which the system is left uncontrolled to reset the original state of STC. The results are shown in Fig. 4, where one sees that the system is able to attain each one of the target pattern in the sequence for the same value of $\gamma = 0.4$, as well as to switch between the different patterns. Notice that each target pattern in the sequence produces a different state in the correlation, depending upon its specific instability features within the uncontrolled STC regime. The maximal correlation is again obtained for the snapshot of the uncontrolled dynamics, since this pattern represents a specific state compatible with the uncontrolled dynamics.

In conclusion we have demonstrated targeting and control over spatiotemporal chaos in an optical feedback loop experiment. Stationary target patterns with arbitrary symmetry and complexity are stabilized in real-time by means of a two dimensional space extended perturbation field at low cost in terms of the perturbation amplitude. The flexibility of the system in switching between different target patterns has also been demonstrated.

Work partly supported by EU Contract HPRN-CT-2000-00158, and MIUR-FIRB project n. RBNE01CW3M-001.

[1] For a comprehensive review of the topic see S. Boccaletti, C. Grebogi, Y.C. Lai, H. Mancini and D. Maza, Phys. Rep. **329**, 103 (2000), and References therein.

[2] I. Aranson, H. Levine and L. Tsimring, Phys. Rev. Lett. **72**, 2561 (1994); W. Lu, D. Yu and R.G. Harrison, Phys. Rev. Lett. **76**, 3316 (1996); R. Martin, A.J. Scroggie, G.L. Oppo and W.J. Firth, Phys. Rev. Lett. **77**, 4007 (1996); N. Baba, A. Amann, E. Scholl, and W. Just Phys. Rev. Lett. **89**, 074101 (2002).

[3] P. Parmananda, M. Hildebrand and M. Eiswirth, Phys. Rev. **E56**, 239 (1997); R.O. Grigoriev, M.C. Cross and H.G. Schuster, Phys. Rev. Lett. **79**, 2795 (1997); L. Kocarev, U. Parlitz, T. Stojanovski and P. Janjic, Phys. Rev. **E 56**, 1238 (1997).

[4] R. Montagne and P. Colet, Phys. Rev. **E56**, 4017 (1997); S. Boccaletti, J. Bragard and F.T. Arecchi, Phys. Rev. **E59**, 6574 (1999).

[5] M. E. Bleich, D. Hochheiser, J.V. Moloney and J.E.S. Socolar, Phys. Rev. **E55**, 2119 (1997); D. Hochheiser, J.V. Moloney and J. Lega, Phys. Rev. **A55**, R4011 (1997).

[6] S.J. Jensen, M. Schwab and C. Denz, Phys. Rev. Lett. **81**, 1614 (1998); T. Ackemann, B. Giese, B. Schäpers and W. Lange, J. Opt. **B1**, 70 (1999); G.K. Harkness, G.L. Oppo, E. Benkler, M. Kreuzer, R. Neubecker and T. Tschudi, J. Opt. **B1**, 177 (1999); E. Benkler, M. Kreuzer, R. Neubecker, T. Tschudi, Phys. Rev. Lett. **84**, 879 (2000).

[7] A.V. Mamaev and M. Saffman, Phys. Rev. Lett, **80**, 3499 (1998).

[8] Akhmanov S.A., Vorontsov M.A. and Ivanov V.Yu., 1988 JETP Lett. **47**, 707. P.L. Ramazza, S. Boccaletti, U Bortolozzo and F.T. Arecchi, Chaos **13**, 335 (2003), and Refs. therein.

[9] G. D'Alessandro and W.J. Firth, Phys. Rev. Lett. **66** 2597 (1991).

[10] Neubecker R., Oppo G.L., Thuering B. and Tschudi T., 1995 Phys. Rev. **A52**, 791.

[11] R. Neubecker, B. Thuring, M. Kreuzer and T. Tschudi, Chaos, Solitons and Fractals **10**, 681 (1999).

[12] B.J. Gluckman, P. Marcq, J. Bridger and J.P. Gollub, Phys. Rev. Lett. **71**, 2034 (1993); Li Ning, Y. Hu, R.E. Ecke and G. Ahlers, Phys. Rev. Lett. **71**, 2216 (1993); E. Bosch, H. Lambermont and W. vandeWater, Phys. Rev. **E49**, R3580 (1994); S. Rudroff and I. Rehberg, Phys. Rev. **E55**, 2742 (1997).